

# Numerical Simulation of Pressure-induced Separation of Turbulent Flat-plate Boundary Layers: Definition and Overview of New Cases with Suction-only Transpiration and a Step in Reynolds Number

*Gary Neil Coleman*  
*Langley Research Center, Hampton, Virginia*

---

September 2021

## NASA STI Program...in Profile

Since its founding, NASA has been dedicated to the advancement of aeronautics and space science. The NASA scientific and technical information (STI) program plays a key part in helping NASA maintain this important role.

The NASA STI Program operates under the auspices of the Agency Chief Information Officer. It collects, organizes, provides for archiving, and disseminates NASA's STI. The NASA STI Program provides access to the NASA Aeronautics and Space Database and its public interface, the NASA Technical Report Server, thus providing one of the largest collection of aeronautical and space science STI in the world. Results are published in both non-NASA channels and by NASA in the NASA STI Report Series, which includes the following report types:

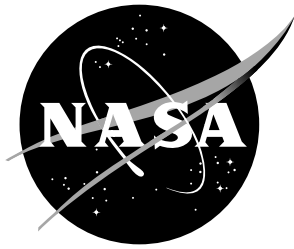
- **TECHNICAL PUBLICATION.** Reports of completed research or a major significant phase of research that present the results of NASA programs and include extensive data or theoretical analysis. Includes compilations of significant scientific and technical data and information deemed to be of continuing reference value. NASA counterpart of peer-reviewed formal professional papers, but having less stringent limitations on manuscript length and extent of graphic presentations.
- **TECHNICAL MEMORANDUM.** Scientific and technical findings that are preliminary or of specialized interest, e.g., quick release reports, working papers, and bibliographies that contain minimal annotation. Does not contain extensive analysis.
- **CONTRACTOR REPORT.** Scientific and technical findings by NASA-sponsored contractors and grantees.

- **CONFERENCE PUBLICATION.** Collected papers from scientific and technical conferences, symposia, seminars, or other meetings sponsored or co-sponsored by NASA.
- **SPECIAL PUBLICATION.** Scientific, technical, or historical information from NASA programs, projects, and missions, often concerned with subjects having substantial public interest.
- **TECHNICAL TRANSLATION.** English-language translations of foreign scientific and technical material pertinent to NASA's mission.

Specialized services also include organizing and publishing research results, distributing specialized research announcements and feeds, providing information desk and personal search support, and enabling data exchange services.

For more information about the NASA STI Program, see the following:

- Access the NASA STI program home page at <http://www.sti.nasa.gov>
- E-mail your question to [help@sti.nasa.gov](mailto:help@sti.nasa.gov)
- Phone the NASA STI Information Desk at 757-864-9658
- Write to:  
NASA STI Information Desk  
Mail Stop 148  
NASA Langley Research Center  
Hampton, VA 23681-2199



# Numerical Simulation of Pressure-induced Separation of Turbulent Flat-plate Boundary Layers: Definition and Overview of New Cases with Suction-only Transpiration and a Step in Reynolds Number

*Gary Neil Coleman*  
*Langley Research Center, Hampton, Virginia*

National Aeronautics and  
Space Administration

Langley Research Center  
Hampton, Virginia 23681-2199

---

September 2021

## Acknowledgments

This work was sponsored by the NASA Transformational Tools and Technologies (TTT) Project of the Transformative Aeronautics Concepts Program under the Aeronautics Research Mission Directorate. Computations were performed on resources provided by the NASA Advanced Supercomputing (NAS) Division. The author is grateful to Dr. David Scott, for the UK/EPSCRC-sponsored code development, and Drs. Christopher Rumsey and Philippe Spalart, for their timely advice and comments.

<p>The use of trademarks or names of manufacturers in this report is for accurate reporting and does not constitute an official endorsement, either expressed or implied, of such products or manufacturers by the National Aeronautics and Space Administration.</p>
---

Available from:

NASA STI Program / Mail Stop 148  
NASA Langley Research Center  
Hampton, VA 23681-2199  
Fax: 757-864-6500

## Abstract

Results from two new direct numerical simulations (DNSs) are added to the database described in Coleman, Rumsey & Spalart (2018) (henceforth CRS18), and available at the NASA TMR website (<https://turbmodels.larc.nasa.gov>). The new flows, Cases D and E, are similar to the earlier ones (Cases A–C) in that a transpiration profile above a flat plate creates a prolonged adverse pressure gradient (APG) that drives a canonical turbulent zero-pressure-gradient (ZPG), flat-plate boundary layer towards separation; they differ in that for the new cases (1) the APG is not followed by a favorable gradient (FPG), since only suction transpiration is employed, and (2) the mean shear stress does not cross zero, so that the width of the mean bubble, strictly defined, is zero. However, the probability of reversed skin friction exceeds 49%. The motivation was to produce a flow more akin to technological flows, including shock-boundary-layer interaction, with a gradual turbulence-controlled recovery. One of the new simulations is also at a significantly higher Reynolds number than the earlier flows.

## Description of new DNS

The fully turbulent incompressible ZPG boundary layer over a flat no-slip surface is subject to streamwise ( $x$ ) pressure gradients induced by a transpiration profile  $V_{\text{top}}(x)$  through a virtual parallel streamwise-spanwise ( $x$ - $z$ ) plane offset a fixed wall-normal distance  $y = Y$  from the no-slip surface. The strength and duration of the pressure gradients are controlled by the maximum velocity  $V_{\text{max}}$  and length-scale  $\sigma$ ; for Cases D and E (cf. (2.1) of CRS18),

$$V_{\text{top}}(x) = V_{\text{max}} \exp \left( - \left[ \frac{x - x_0}{\sigma} \right]^2 \right) + \varphi_{\text{top}} g(x) + \Phi(x), \quad (1)$$

where  $x_0$  sets the location of the peak  $V_{\text{top}}$ ,  $\varphi_{\text{top}}$  is a small ‘bleed’ velocity, adjusted to offset the blockage in the (nominally) ZPG regions upstream of separation, and thereby produce  $dP/dx \approx 0$  along the wall there; the bleed velocity is constant for  $x < x_\varphi$  and zero for  $x > x_\varphi$ , since  $g(x) = 0.5(1 - \text{erf}((x - x_\varphi)/\sigma_\varphi))$ . We use  $x_\varphi = 15.35$  and  $\sigma_\varphi = \sigma/10$  for both cases. The transpiration is very similar to that of Alam & Sandham (2000) and Spalart & Strelets (2000), although both those studies had a laminar incoming boundary layer, and Wu, Meneveau & Mittal (2020). The inflow/outflow boundary conditions are imposed by the fringe-zone treatment described in CRS18, which allows a fully spectral spatial scheme to accommodate the spatially developing, nonparallel flow. The fringe parameters given in Table 3 of CRS18 ( $x_1$ ,  $V_2$ ,  $y_\alpha$ ,  $\Upsilon$ ,  $y_\beta$ ), along with (A1) and (A2) of CRS18, are also used for Cases D and E. The last term in (1) maintains zero net mass flux across the  $y = Y$  plane, by injecting mass into the fringe zones (and only there):  $\Phi(x) = -(V_{\text{max}}\sigma/x_1 + \varphi_{\text{top}}x_\varphi/\sqrt{\pi}x_1)H(x)$ , where  $H(x) = \exp(-(x/x_1)^2) + \exp(-((x - \Lambda_x)/x_2)^2)$ . Other numerical details are as given in CRS18.

Table 1. Case parameters.

Case	$U_\infty Y/\nu$	$V_{\max}/U_\infty$	$x_0/Y$	$\sigma/Y$	$\varphi_{\text{top}}/U_\infty$
D	80 000	0.125	12.762	2.407	0.0032
E	180 000	0.125	12.762	2.407	0.0032

The cases are summarized in Table 1. Case D is at the same Reynolds number as the previous Case C, whereas the Reynolds number of Case E is more than twice as high. Figure 1 illustrates the qualitative differences between the new suction-only cases (dashed and solid curves) and the earlier APG/FPG flows (the chain-dotted curves are from Case C of CRS18). Note the weak APG (replacing a strong FPG), and continued growth of the boundary layer, downstream of the  $V_{\text{top}} > 0$  region. Mean-flow contours and streamlines for Case E are shown in Figure 2. The ‘hotspot’ in the Reynolds shear stress  $-\overline{u'v'}$  near  $x = 21$  (Figure 2b) is qualitatively similar to that observed in the NASA wall-mounted hump experiment (Greenblatt et al. 2006a,b; Naughton et al. 2006), although here it is milder: compared to the peak value found in the experiment of about  $0.03(\Delta U)^2$  (where  $\Delta U$  is the velocity difference across the effective shear layer within which the hotspot is embedded), the Case E equivalent is  $-\overline{u'v'} \approx 0.01(\Delta U)^2$ . The latter is similar to the value in a plane mixing layer, and therefore there is some expectation that turbulence models may reproduce it, provided the growth from the much lower levels typical of boundary layers is rapid enough.

We interpret the  $x/Y = 7.5$  station as the ZPG reference states. At these locations, the Case D and E flows both agree well with ZPG boundary-layer results from DNS and experiment, in terms of mean velocity at momentum thickness Reynolds numbers of 1479 and 3069 (Figure 3). The profiles of near-wall turbulence kinetic energy and terms in its budget (neither shown) also agree well with Schlatter & Örlü’s (2010) DNS at comparable  $R_\theta$ . In the outer layer, the Case E profile is somewhat more energetic than the pure ZPG DNS benchmark at the same  $y^+$  location (cf. Figure 6 of CRS18, regarding Case C).

The numerical parameters are summarized in Table 2; in general they meet the standard required of a DNS (cf. § 2.2 of CRS18): the spatial resolution is quite close to that used in CRS18, and all scales are fully captured throughout most of the domain. The exception (as in CRS18) is the marginal accommodation of the residual vorticity near the top wall, associated with the layer thickness approaching the transpiration plane – which in CRS18 resulted in minor near-wall oscillation (Gibbs phenomenon) in the profiles above the separation bubble (see Figure 4 of CRS18). The present Figure 4 shows mean and root-mean-square (RMS) fluctuations of vorticity at several  $x$ -stations. At upstream stations ( $x/Y = 7.5$  shown here), the profiles decay cleanly to zero well below the upper, transpiration boundary. But starting near  $x/Y = 15$  and extending downstream ( $x/Y = 15$  and 23 are shown), nonzero levels of  $\overline{\omega}_z$  and  $\overline{\omega'_i \omega'_i}^{1/2}$  are evident near the upper boundary. These nonzero levels extend from near  $x/Y = 15$  (where the skin friction is smallest) until the outflow station, where for both new cases the RMS vertical velocity fluc-

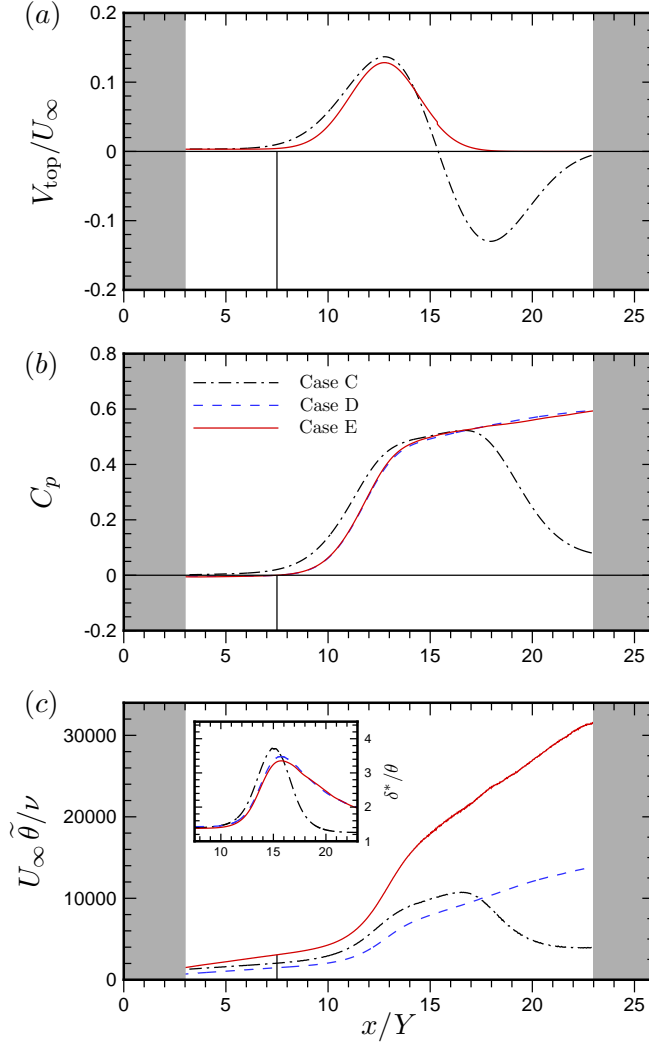


Figure 1. Streamwise variation of (a) transpiration profile along  $y = Y$ , (b) mean wall pressure and (c) momentum-thickness Reynolds number and shape factor. Case D and E results are identical in (a). Vertical lines mark the assumed ZPG reference station for Cases D and E. Shaded rectangles (approximately  $3Y$  wide) indicate regions where the fringe/inflow-treatment is active for Cases D and E. (For Case C, the effective fringe regions are each approximately  $2Y$  wide, since the boundary layer to which the fringe forcing is applied is thinner in that flow, due to its FPG downstream of separation.)

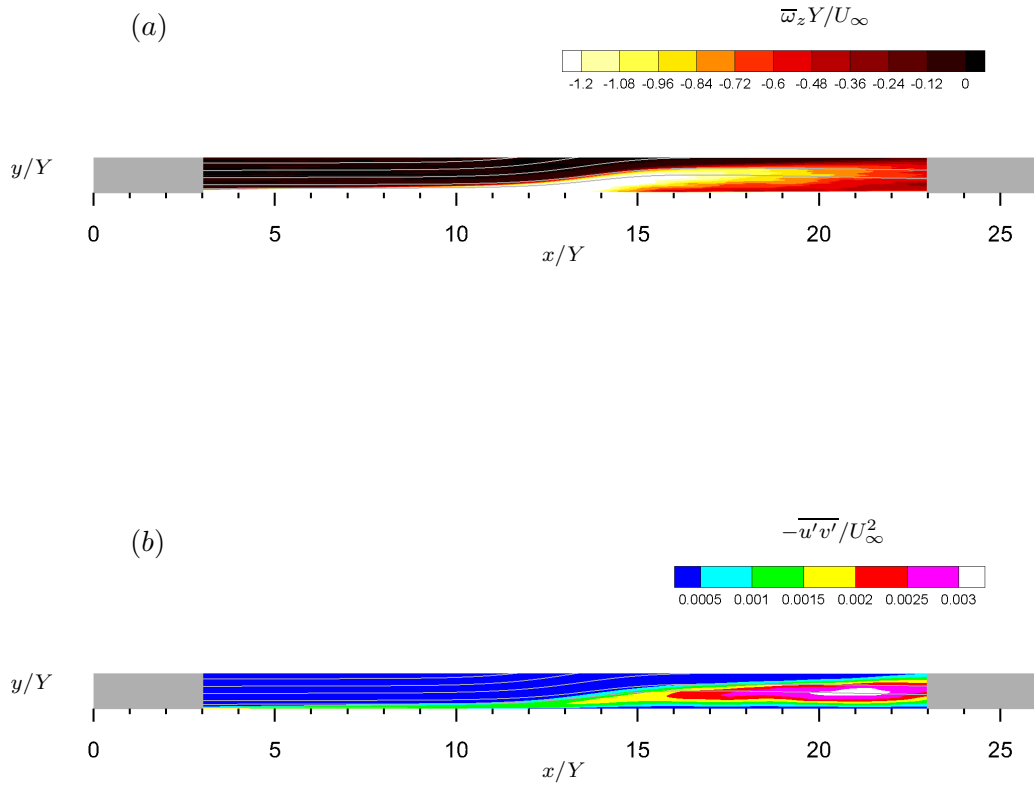


Figure 2. Contours of mean streamlines and (a) spanwise vorticity  $\bar{\omega}_z$  and (b) Reynolds shear stress  $-\overline{u'v'}$  for Case E. Shaded/grey regions in in/outflow of domain are fringe zones.



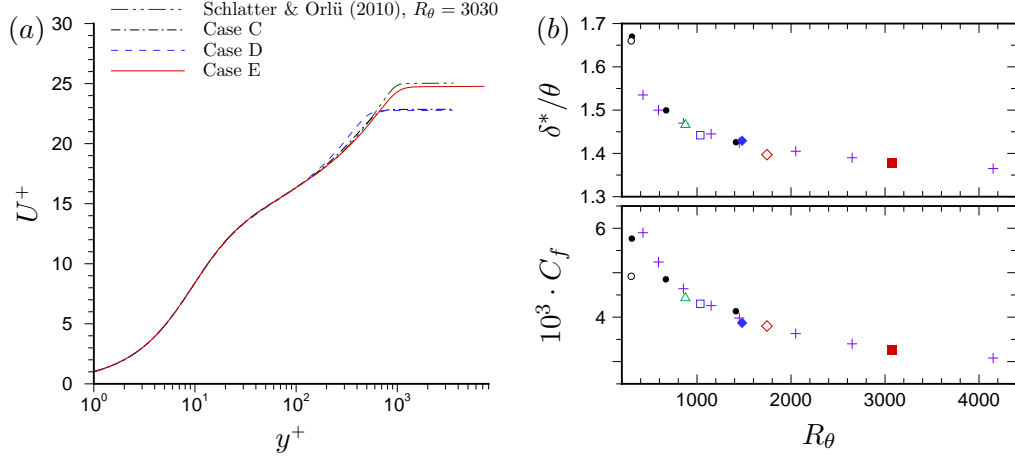


Figure 3. (a) Mean-velocity in ZPG regions. (b) Skin-friction and shape factor: +, Coles (1962); •, Spalart (1988); ◦, SC97; ◻, Case A; ◄, Case B; ◊, Case C; ◆, Case D; ■, Case E.

Table 2. Numerical parameters. Dealiasing is enforced by defining the number of quadrature/collocation points,  $N_x$ ,  $N_y$  and  $N_z$ , such that they are related to the number of streamwise, wall-normal and spanwise Galerkin spectral expansion coefficients, respectively, by  $M_x = 2N_x/3$ ,  $M_y = (2N_y - 9)/3$  and  $M_z = 2N_z/3$ . Spatial resolution is quantified in terms of the quadrature grid, such that  $\Delta x = \Lambda_x/N_x$  and  $\Delta z = \Lambda_z/N_z$ , where  $\Lambda_x$  and  $\Lambda_z$  are respectively streamwise and spanwise domain periods. The distance  $y_{10}$  is that of the tenth wall-normal quadrature point from the bottom of the domain (with  $y_1 = 0$ ). Wall units, e.g.,  $\Delta x^+ = \Delta x u_\tau/\nu$  and  $y_{10}^+ = y_{10} u_\tau/\nu$ , are based on skin friction at  $x/Y = 3$ .

Case	$\Lambda_x/Y$	$\Lambda_z/Y$	$N_x$	$\Delta x^+$	$N_y$	$y_{10}^+$	$N_z$	$\Delta z^+$
C	26.0	4.0	7680	12.3	240	4.6	2560	5.7
D	26.0	4.0	7680	13.4	240	5.0	2560	6.2
E	26.0	4.0	18 432	11.6	320	5.8	6400	5.1

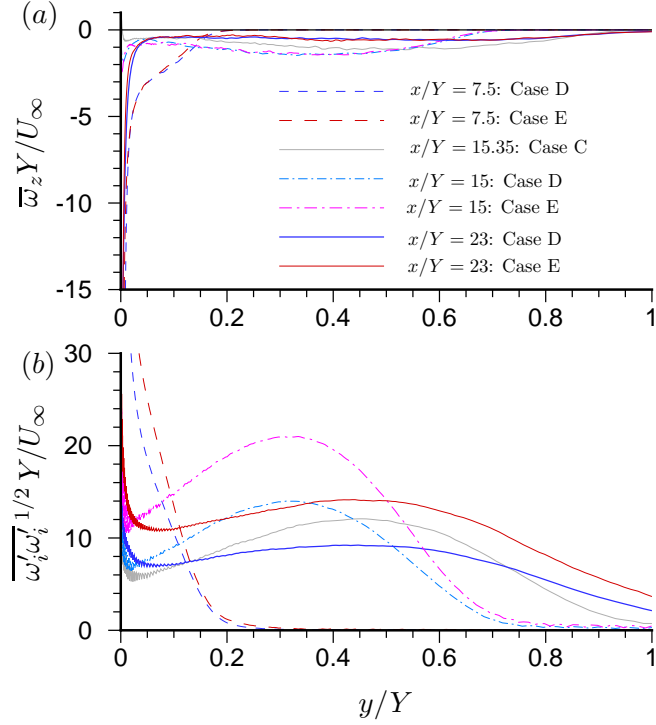


Figure 4. Profiles of (a) mean spanwise vorticity  $\overline{\omega}_z$  and (b) root-mean-square vorticity fluctuations  $\overline{\omega'_i \omega'_i}^{1/2}$ .

tuations (not shown) are approximately  $0.025U_\infty$  at  $y = Y$ , compared with a peak value of about 0.064 (near  $y = 0.45Y$ ). As was true for Cases A, B, and C, although the vorticity oscillations are relatively small, this implies certain statistics (such as the dissipation term in the turbulence-kinetic-energy budget) should be viewed with caution in the affected regions, downstream of the minimum skin-friction station.

The parameters of the transpiration profile were adjusted to drive the layer just to the point of mean separation, near  $x/Y = 15$ , before allowing the flow to recover under nominally ZPG conditions before exiting/reentering the domain through the fringe zones (Figures 1 and 5a). The mean-velocity profile evolves in the downstream  $V_{\text{top}} = 0$  region such that a mild APG ensues (see the shape-factor  $\delta^*/\theta$  profile in Figure 1c). Despite the skin friction just ‘kissing’  $C_f = 0$  before growing again, the structure of the near-wall turbulence under the APG is qualitatively similar to flows for which a finite separation bubble forms. This can be seen by comparing Figure 6 with Figure 1d of CRS18. This underlines the oft-made observation that the flow does not fundamentally change once it passes the mean  $C_f = 0$  location, which also closely corresponds to the 50% back-flow station (Figure 5b). Figure 5b also demonstrates the tendency for the small but nonzero number of instantaneous reversed-flow events at the wall under the ZPG layer (e.g. at  $x/Y = 7.5$ ) to increase with Reynolds number (Spalart 1988).

Statistics were gathered by averaging over  $z$  and in time, involving 381 and 763  $x$ - $y$  fields over periods of  $35.1$  and  $16.35Y/U_\infty$ , respectively, for Cases D and

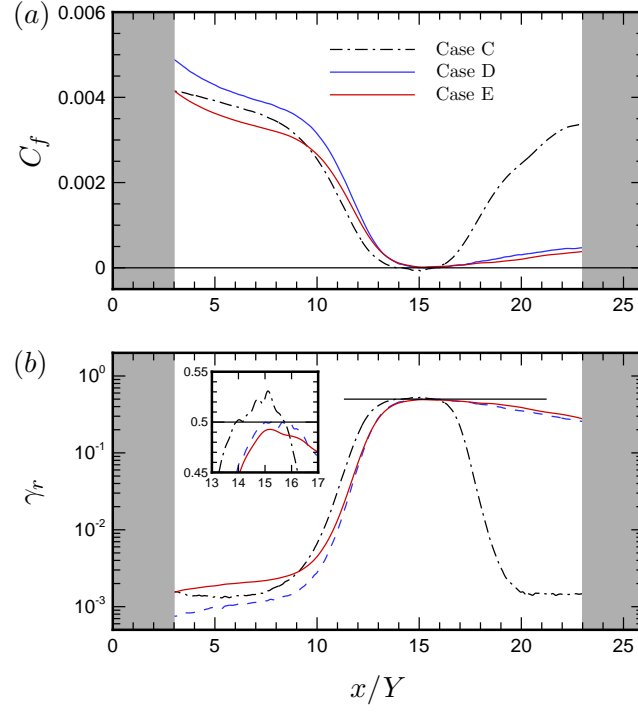


Figure 5. (a) Skin-friction  $C_f = \tau_w / \frac{1}{2} \rho U_\infty^2$  and (b) fraction of reversed wall shear  $\gamma_r$ . Horizontal lines in (b) denote  $\gamma_r = 0.50$  threshold.

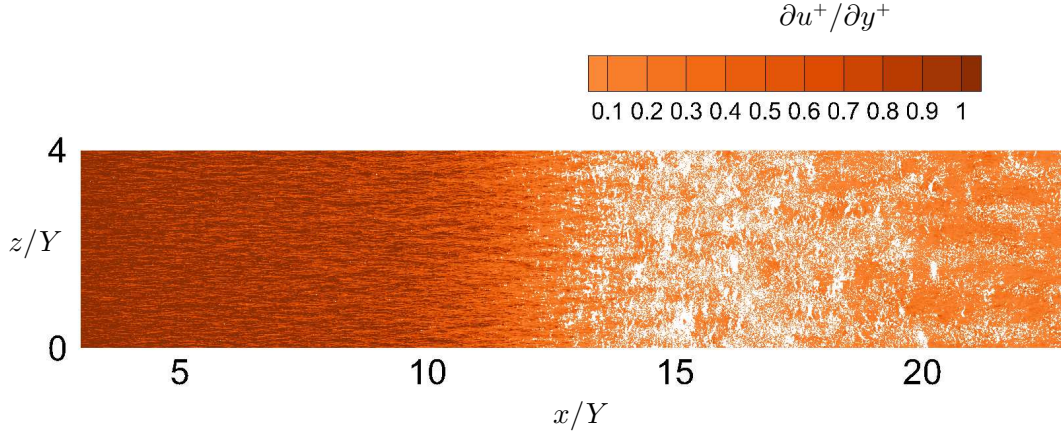


Figure 6. Contours of instantaneous surface shear stress for Case D. White contours denote  $\partial u / \partial y < 0$ .

E (respectively corresponding to 1.35 and 0.6 domain-flow-through times  $\Lambda_x/U_\infty$ ). Some quantities were also locally averaged in  $x$ . The  $z$ - and  $t$ -averaged data are available from the NASA Turbulence Modeling Resource (TMR) website.<sup>1</sup>

Computations were done on the NASA Advanced Supercomputing (NAS) Division’s Aitken AMD Rome system, on 4096 cores. A total of about 245,000 (Case D) and 2,561,000 (Case E) CPU-core-hours were utilized during the statistics-gatherings phase of the computations.

## Closing comments

Taken in tandem with CRS18, these new DNS data are expected to aid understanding of canonical smooth-body separation driven by APG. The new data provide a different type of recovery from separation (gentle APG rather than FPG), and also include two different Reynolds numbers.

## References

- ALAM, M. & SANDHAM, N. D. 2000 Direct numerical simulation of ‘short’ laminar separation bubbles with turbulent reattachment. *J. Fluid Mech.* **410**, 1–28.
- COLES, D. E. 1962 The turbulent boundary layer in a compressible fluid. *Rand Rep.* R403-PR, ARC 24473: Appendix A: A manual of experimental practice for low-speed flow.
- GREENBLATT, D., PASCHAL, K. B., YAO, C.-S., HARRIS, J., SCHAEFFLER, N. W. & WASHBURN, A. E. 2006a Experimental investigation of separation control Part 1: Baseline and steady suction. *AIAA J.* **44**(12), 2820–2830.
- GREENBLATT, D., PASCHAL, K. B., YAO, C.-S. & HARRIS, J. 2006b Experimental investigation of separation control Part 2: Zero mass-flux oscillatory blowing. *AIAA J.* **44**(12), 2831–2845.
- NAUGHTON, J. W., VIKEN, S. A. & GREENBLATT, D. 2006 Skin-friction measurements on the NASA hump model. *AIAA J.* **44**(6), 1255–1265.
- SCHLATTER, P. & ÖRLÜ 2010 Assessment of direct numerical simulation data of turbulent boundary layers. *J. Fluid Mech.* **659**, 116–126.
- SPALART, P.R. 1988 Direct simulation of a turbulent boundary layer up to  $R_\theta = 1410$ . *J. Fluid Mech.* **187**, 61–98.
- SPALART, P.R. & STRELETS, M. KH. 2000 Mechanisms of transition and heat transfer in a separation bubble. *J. Fluid Mech.* **403**, 329–349.
- WU, W., MENEVEAU, C. & MITTAL, R. 2020 Spatio-temporal dynamics of turbulent separation bubbles. *J. Fluid Mech.* **883**, A45.

---

<sup>1</sup><https://turbmodels.larc.nasa.gov> .

REPORT DOCUMENTATION PAGE					Form Approved OMB No. 0704-0188	
<p>The public reporting burden for this collection of information is estimated to average 1 hour per response, including the time for reviewing instructions, searching existing data sources, gathering and maintaining the data needed, and completing and reviewing the collection of information. Send comments regarding this burden estimate or any other aspect of this collection of information, including suggestions for reducing this burden, to Department of Defense, Washington Headquarters Services, Directorate for Information Operations and Reports (0704-0188), 1215 Jefferson Davis Highway, Suite 1204, Arlington, VA 22202-4302. Respondents should be aware that notwithstanding any other provision of law, no person shall be subject to any penalty for failing to comply with a collection of information if it does not display a currently valid OMB control number.</p> <p><b>PLEASE DO NOT RETURN YOUR FORM TO THE ABOVE ADDRESS.</b></p>						
1. REPORT DATE (DD-MM-YYYY) 01-09-2021		2. REPORT TYPE Technical Memorandum		3. DATES COVERED (From - To)		
4. TITLE AND SUBTITLE Numerical Simulation of Pressure-induced Separation of Turbulent Flat-plate Boundary Layers: Definition and Overview of New Cases with Suction-only Transpiration and a Step in Reynolds Number				5a. CONTRACT NUMBER		
				5b. GRANT NUMBER		
				5c. PROGRAM ELEMENT NUMBER		
6. AUTHOR(S) G. N. Coleman				5d. PROJECT NUMBER		
				5e. TASK NUMBER		
				5f. WORK UNIT NUMBER 109492.02.07.05.01		
7. PERFORMING ORGANIZATION NAME(S) AND ADDRESS(ES) NASA Langley Research Center Hampton, Virginia 23681-2199				8. PERFORMING ORGANIZATION REPORT NUMBER		
9. SPONSORING/MONITORING AGENCY NAME(S) AND ADDRESS(ES) National Aeronautics and Space Administration Washington, DC 20546-0001				10. SPONSOR/MONITOR'S ACRONYM(S) NASA		
				11. SPONSOR/MONITOR'S REPORT NUMBER(S) NASA/TM-20210020762		
12. DISTRIBUTION/AVAILABILITY STATEMENT Unclassified-Unlimited Subject Category Availability: NASA STI Program (757) 864-9658						
13. SUPPLEMENTARY NOTES An electronic version can be found at <a href="http://ntrs.nasa.gov">http://ntrs.nasa.gov</a> .						
14. ABSTRACT Results from two new direct numerical simulations (DNSs) are added to the database described in Coleman, Rumsey & Spalart (2018) (henceforth CRS18), and available at the NASA TMR website ( <a href="https://turbmodels.larc.nasa.gov">https://turbmodels.larc.nasa.gov</a> ). The new flows, Cases D and E, are similar to the earlier ones (Cases A-C) in that a transpiration profile above a flat plate creates a prolonged adverse pressure gradient (APG) that drives a canonical turbulent zero-pressure-gradient (ZPG), flat-plate boundary layer towards separation; they differ in that for the new cases (1) the APG is not followed by a favorable gradient (FPG), since only suction transpiration is employed, and (2) the mean shear stress does not cross zero, so that the width of the mean bubble, strictly defined, is zero. However, the probability of reversed skin friction exceeds 49%. The motivation was to produce a flow more akin to technological flows, including shock-boundary-layer interaction, with a gradual turbulence-controlled recovery. One of the new simulations is also at a significantly higher Reynolds number than the earlier flows.						
15. SUBJECT TERMS Direct numerical simulation, turbulent boundary layer, adverse pressure gradient, separation						
16. SECURITY CLASSIFICATION OF:			17. LIMITATION OF ABSTRACT	18. NUMBER OF PAGES	19a. NAME OF RESPONSIBLE PERSON	
a. REPORT	b. ABSTRACT	c. THIS PAGE			STI Information Desk ( <a href="mailto:help@sti.nasa.gov">help@sti.nasa.gov</a> )	
U	U	U	UU	13	19b. TELEPHONE NUMBER (Include area code) (757) 864-9658	